

Supporting Information

Electrical Chiral Assembly Switching of Soluble
Conjugated Polymers from
Propylenedioxythiophene-Phenylene Copolymers

*Xu Yang, Seogjae Seo, Chihyun Park and Eunkyong Kim**

TABLE OF CONTENTS

1. Experimental Section
2. Characterization of YPCr monomers and polymer (Figure S1-S4)
3. Thickness dependence of YPCr films (Figure S5)
4. Differential scanning calorimetry (DSC) of YPCr (Figure S6)
5. Morphologies of as-prepared and annealed YPCr film (Figure S7, Table S1)
6. X-ray diffraction (XRD) of YPCr films in different states (Figure S8)

7. Morphology and thickness changes of YPCr films during electrochemical processing (Figure S9-10)
8. UV/Vis absorbance spectra YPCr electrochromic device with different doping states (Figure S11)
9. CD, UV/vis absorbance and fluorescence switching of as-prepared YPCr EC device and memory effect (Figure S12)
10. Comparison of electrochemical properties from YPCr and other reported references (Table S2)
11. Electrochemical switching properties of YPCr under different applied potentials (Table S3)
12. Electrochemical switching properties of YPCr in different thickness (Table S4)
13. Reference for supporting information

Experimental Section

Materials. All the reagents and solvents were purchased from Aldrich Chemicals and used without further purification. ITO glass (sheet resistance, R_s 8-12 Ω sq^{-1}) was purchased from NanoTS Co., Ltd. Ag wire used as a reference electrode was purchased from Dasom RMS.

Instrumentation. The $^1\text{H-NMR}$ was obtained with a Bruker 300 MHz. The average molecular weight of the polymer was characterized by gel permeation chromatography (GPC) (model: Waters R-401 ALC/GPC) with THF as an eluent and a polystyrene standard for calibration. The thickness of the films was determined via profilometry measurements using an Alpha Step

profilometer (Tencor Instruments, Alpha-Step IQ) and cross images from a scanning electron microscope (JSM-7001F, JEOL.). The UV/Vis absorbance and circular dichroism (CD) spectra were characterized with a circular dichroism spectrometer (Jasco J-815). The electrochemical measurements were carried out with an electrochemical analyser (CH Instruments Inc., CHI624B). Fluorescence was measured with a luminescence spectrometer (Perkin-Elmer, Model LS55). Differential scanning calorimetry (DSC) measurements were performed on a Netzsch/DSC 200 F3 at a heating rate of 10 °C/min under a nitrogen atmosphere. Samples were placed in an aluminium pen, sealed tightly, and scanned from 20 °C to 200°C. Atomic force microscopy (AFM) was carried out in tapping mode at room temperature with a Dimension 3100 SPM equipped with a Nanoscope IVa (Digital Instruments, Santa Barbara, CA). Transmission electron microscopy (TEM) images were taken with a high-resolution transmission electron microscopy (HR-TEM) system (JEOL, Model JEM-3010). The photographic images of the electrochromic and fluorescent films were examined with a digital camera (Canon Power Shot D60). The fluorescence quantum yields were determined using a quinine sulfate in H₂SO₄ water solution, as a reference ($\Phi_{\text{ref}} = 0.55$). X-ray diffraction (XRD) was detected by RIGAKU Ultima IV.

Polymer synthesis. 3,3-bis(Bromomethyl)-3,4-dihydro-2H-thieno[3,4-b][1,4]dioxepine (ProDOT-(CH₂Br)₂, **2**) was synthesized from 3,4-dimethoxythiophene (**1**) and 2,2-bis(bromomethyl) propane-1,3-diol with p-toluenesulfonic acid in toluene as a solvent. The resulting mixture was heated to reflux for 24 hour. [¹H NMR (400 MHz, CDCl₃, δ): 6.50 (s, 2H, ArH); 4.09 (m, 4H, CH₂); 3.61 (t, 4H, CH₂).] (**Figure S1**). Compound **3** was synthesized from compound **2** and (*S*)-(-)-2-Methyl-1-butanol in DMF as a solvent, and NaH was added to the mixture. After 1 day of string at 100 °C, the product was extracted with chloroform, and then the

combined organic layers were dried with by rotary evaporator. The product was purified by column chromatography. [^1H NMR (400 MHz, CDCl_3 , δ): 6.47 (s, 2H, ArH); 4.00 (s, 4H, CH_2); 3.48 (s, 4H, CH_2); 3.20 (d, 4H, CH_2); 1.6~1.25 (m, 6H, CH, CH_2); 0.90~0.86 (m, 12H, CH_3)] (**Figure S2**). The monomer **4** (DBProDOT- $(\text{CH}_2\text{OCr})_2$) was prepared by bromination of **3** with N-bromosuccinimide (NBS), and then purified by column chromatography. [^1H NMR (400 MHz, CDCl_3 , δ): 4.08 (s, 4H, CH_2); 3.48 (s, 4H, CH_2); 3.22 (d, 4H, CH_2); 1.62~1.09 (m, 6H, CH, CH_2); 0.90~0.86 (m, 12H, CH_3)] (**Figure S3**). The yellow chiral polymer (YPCr) was synthesized by Suzuki coupling reaction²⁻⁴ from the thiophene monomer **4** and 4,4,5,5-tetramethyl-2-(4-(4,4,5,5-tetramethyl-1,3,2-dioxaborolan-2-yl)phenyl)-1,3,2-dioxaborolane with $\text{P}(\text{o-tol})_3$ in the presence of Pd_2dba_3 (1 mol% Pd/Br), producing a yellow solid polymer with a 70 % yield. GPC Mw = 6600, PDI = 1.40. ^1H NMR (CDCl_3): δ 7.77 (br s, 4H), 4.2 (br s, 4H), 3.60 (br s, 4H), 3.28 (br s, 4H), 1.6-1.2 (br, 6H), 0.90 (br s, 12H) (**Figure S4**).

Sample preparation. Polymer thin films were prepared by spin-coating on ITO glass, silicon wafer and carbon-coated TEM grids for electrochromic, circular dichroism, fluorescence, AFM and TEM measurements, respectively. Film thickness was controlled by changing the spinning speeds and concentrations of the copolymer solutions. Polymer films were annealed at 50, 70, 100, and 120 °C and then slowly cooled to room temperature in air. For the TEM measurements, the specimens were stained by exposing them to Ruthenium tetroxide (RuO_4) vapor for 30 min. Because RuO_4 reacts preferentially with the unsaturated carbon double bonds of thiophene and benzene, the stained thiophene and benzene phase appears dark in a bright-field TEM micrographs.¹

Scheme S1. Synthesis of the yellow chiral polymer.

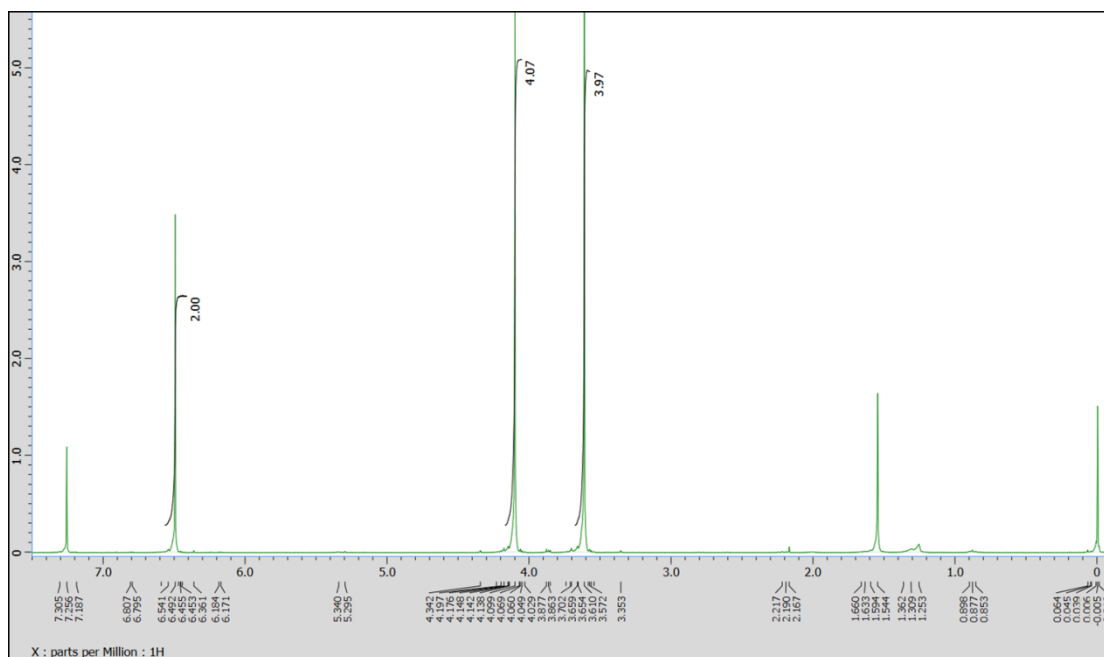
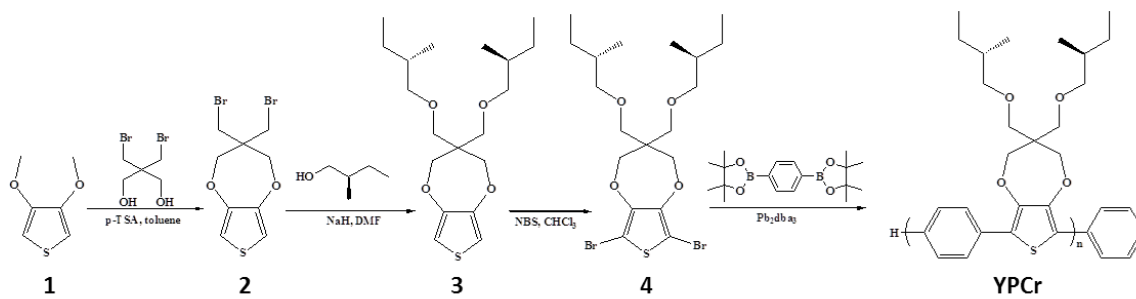


Figure S1. ^1H NMR spectrum of the compound **2** in CDCl_3 .

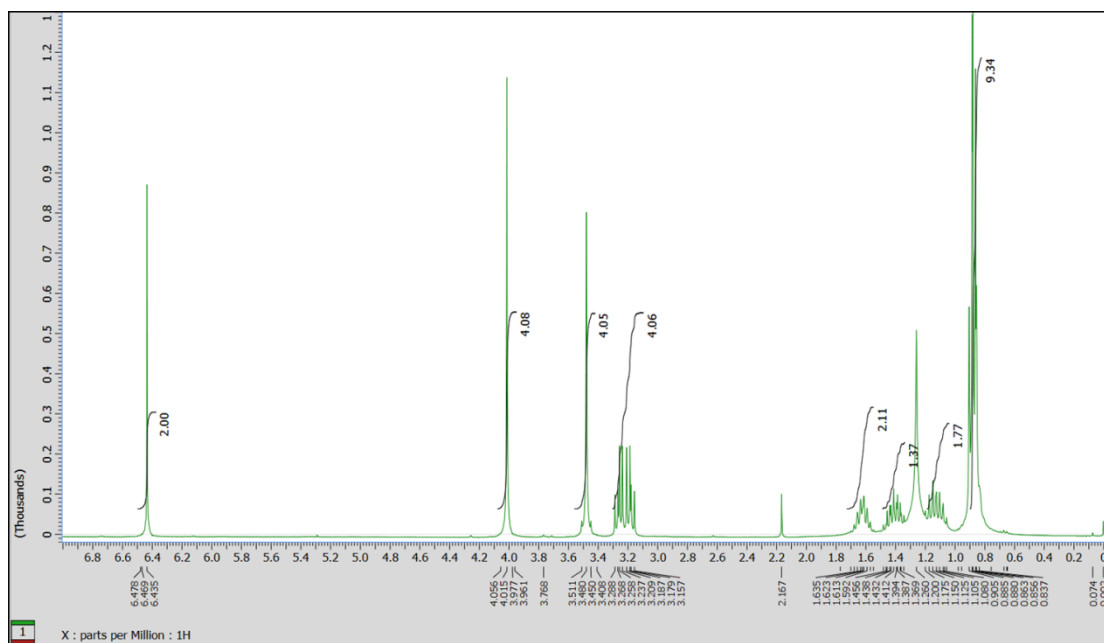


Figure S2. ^1H NMR spectrum of the compound **3** in CDCl_3 .

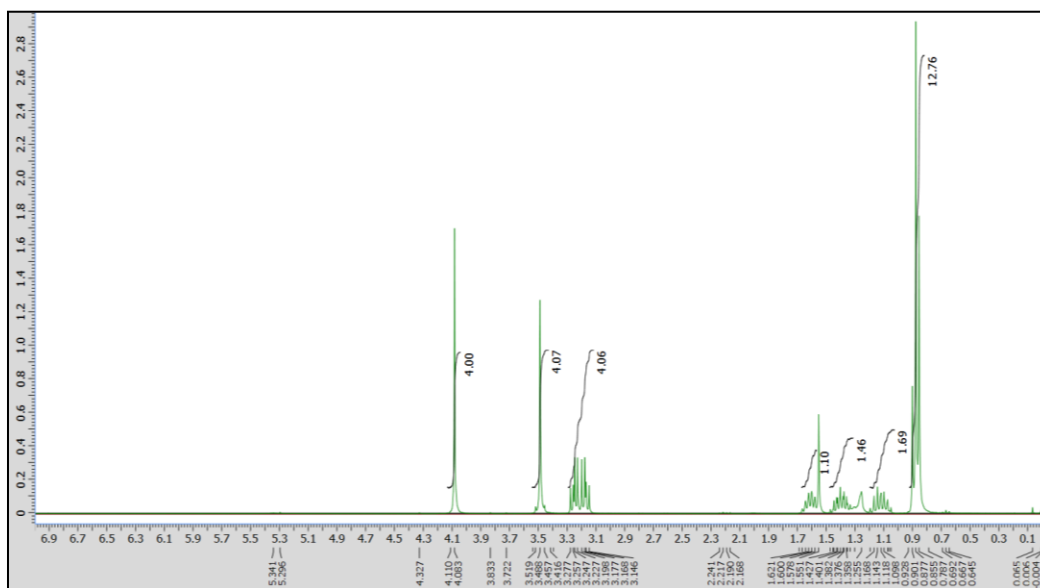


Figure S3. ^1H NMR spectrum of the compound **4** in CDCl_3 .

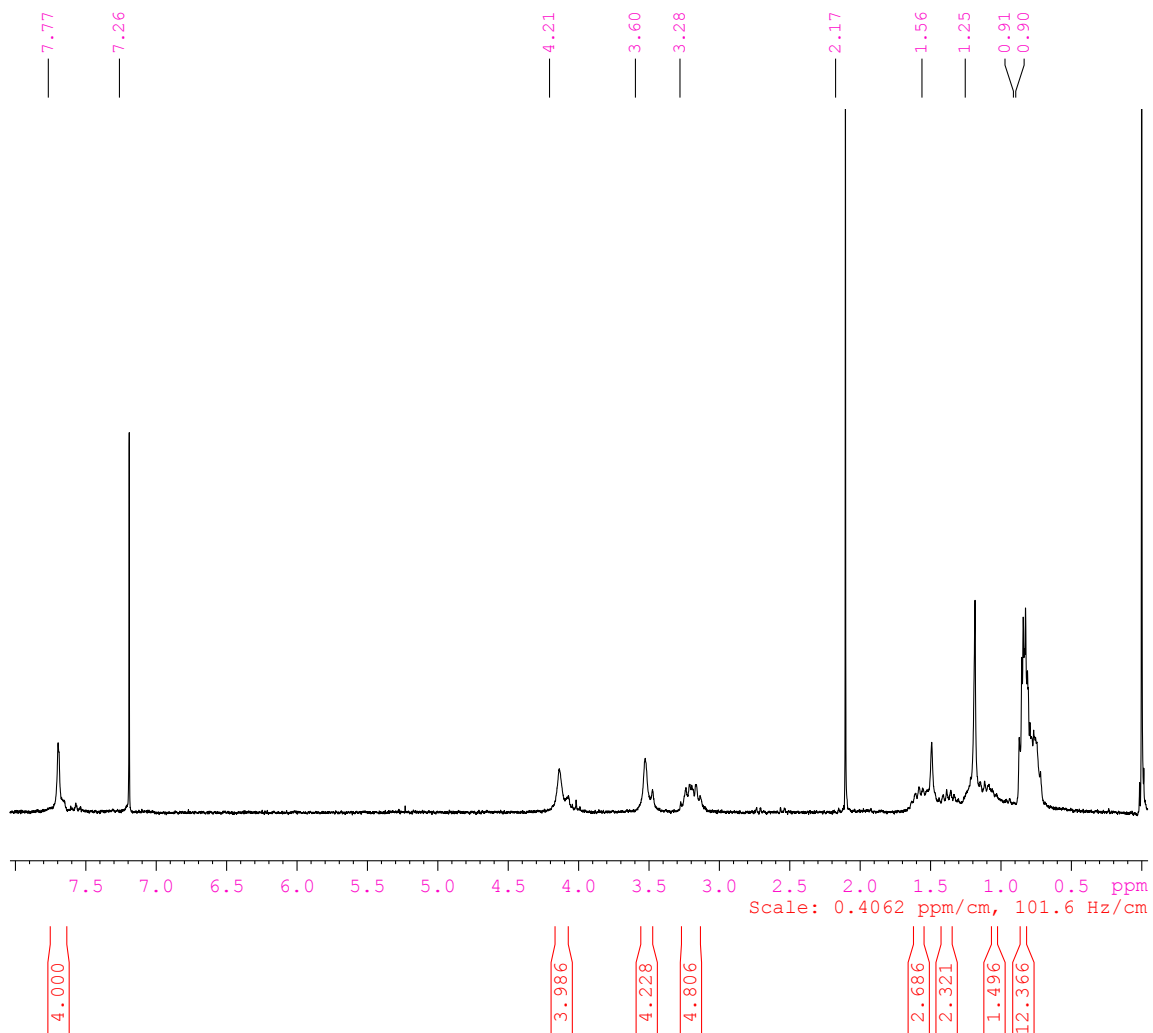


Figure S4. ^1H NMR spectrum of the YPCr polymer in CDCl_3 .

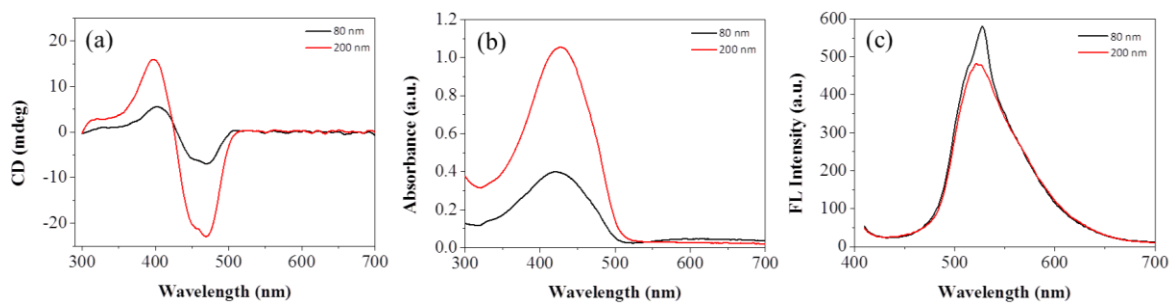


Figure S5. (a) CD, (b) absorbance and (c) fluorescence spectra of the YPCr film at different thicknesses.

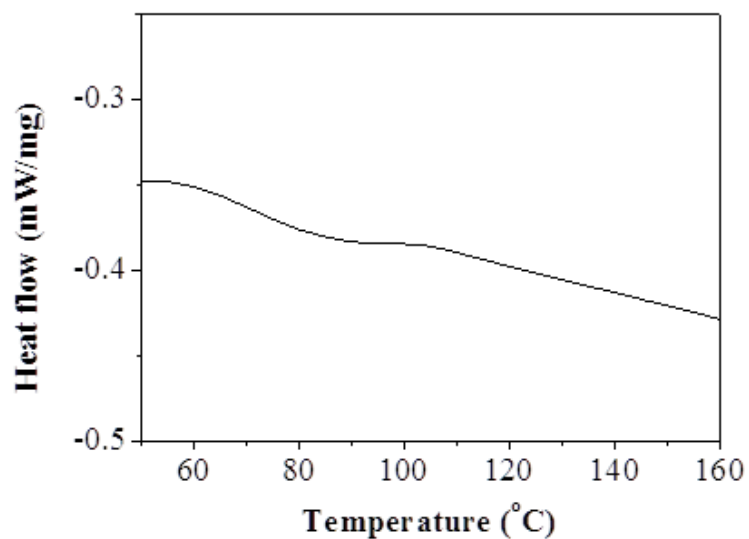


Figure S6. DSC thermogram of the YPCr (scan rate: 20°C/min).

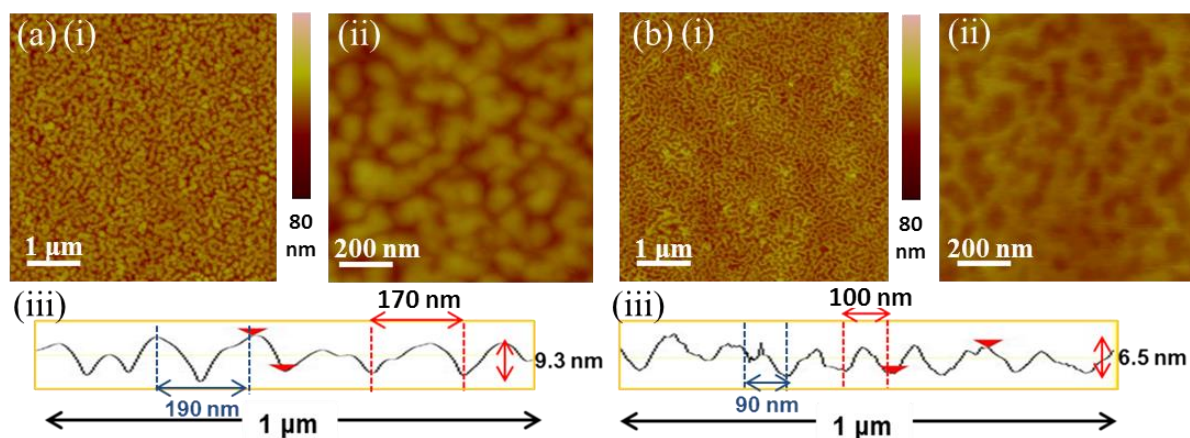


Figure S7. AFM images of the YPCr films (a) as prepared and (b) after annealing at 120 °C. (i) And (ii) present 5x5 μm^2 and 1x1 μm^2 scale, respectively. (iii) The cross height profile of the 1x1 μm^2 scale image, respectively.

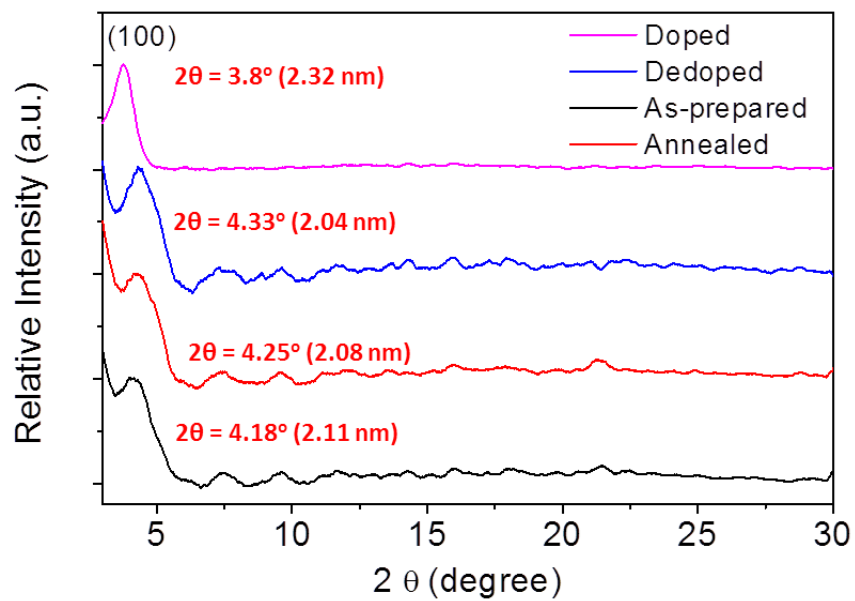


Figure S8. XRD spectra of the YPCr film at as-prepared, annealed, dedoped and doped state on the ITO glass.

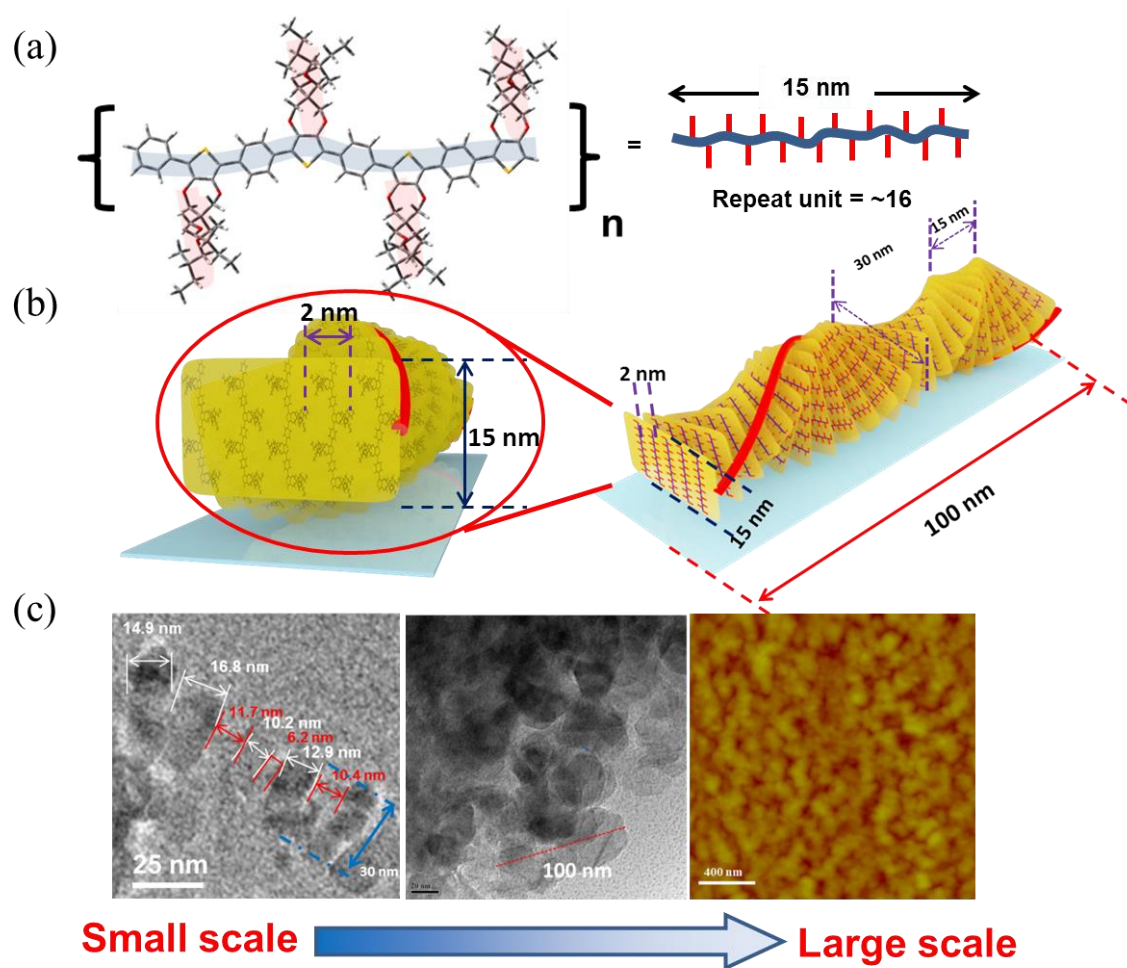


Figure S9. (a) Chemical structure of YPCr and (b) the packing model of YPCr helical structure. (c) The YPCr chiral assembly was observed in small scale TEM images and large scale AFM images with consistently ~ 90 nm lengths.

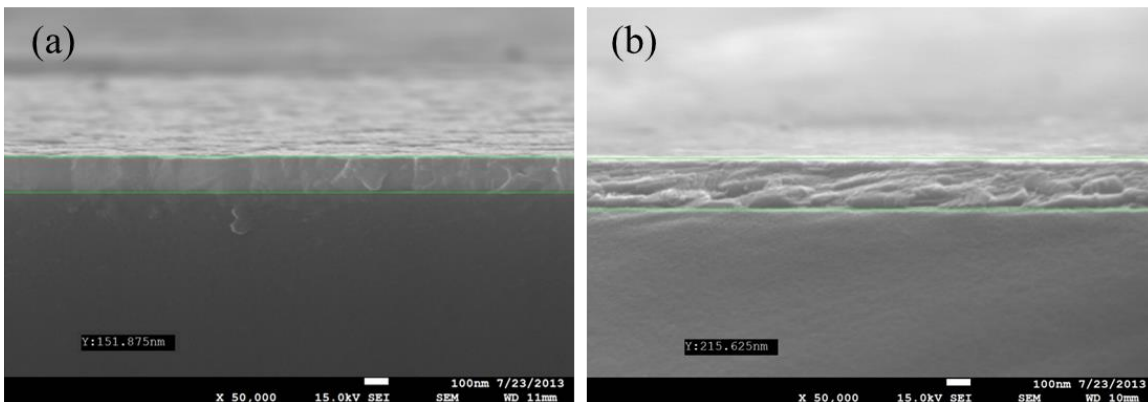


Figure S10. SEM cross-sectional images of YPCr films at (a) dedoped state (0 V) and (b) doped state (+1 V)

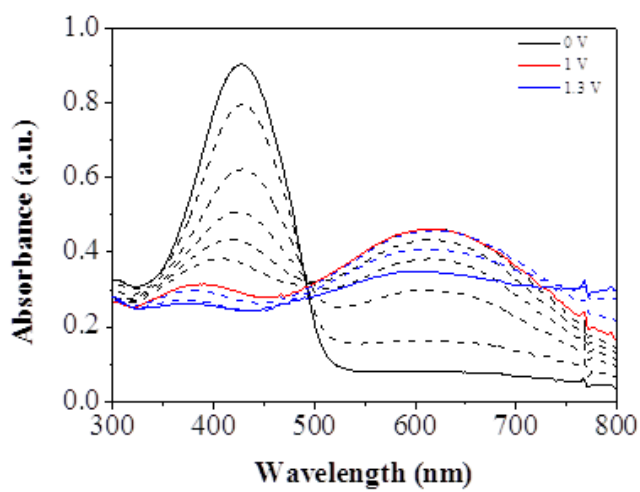


Figure S11. UV/Vis absorbance spectra YPCr electrochromic device with different doping states (black: 0 V, red: 1 V, blue: 1.3 V).

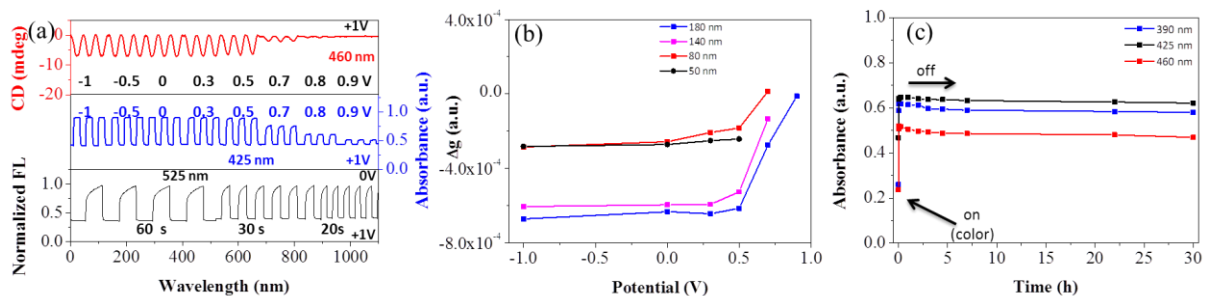


Figure S12. CD (at 460 nm, red), UV/Vis absorbance (blue, at 425 nm) and fluorescence (at 525 nm, black) switching response of the EC device made from the as-prepared YPCr. (b) Δg_{abs} of the annealed YPCr EC device with different thicknesses during the electrochemical redox process, monitored at 460 nm, when the doping potential was fixed at +1 V and dedoping potential was various from -1 V to 0.9 V. (c) The optical long-term memory effect of YPCr device without electricity at three different wavelengths.

Table S1. Water and ethylene glycol contact angle on the YPCr film surface at the different annealing temperatures, and the surface energy of the film.

Annealing temperature [°C]	Contact angle in water [°]	Contact angle in ethylene glycol [°]	Surface energy [mN m ⁻¹] ^{a)}
50	117 	104 	7
120 for 2 h	103 	87 	14
120 for 12h	105 	86 	15

^{a)} Surface energies were calculated using a geometric-mean approach by the Fowkes' method.

Table S2. The chiroptical switching properties of the chiral conjugated polymers with the different preparation and doping methods. The properties of YPCr are compared with other previous reports.

(Materials)	polymerization	Chiral dopant	λ [nm]	CD [mdeg]			Absorbance			Anisotropy factor $g_{abs} \times 10^{-3}$				Ref.
				CD ^{a)}	CD ^{b)}	Δ CD ^{c)}	Abs. ^{a)}	Abs. ^{b)}	Δ Abs	$g_{abs}^{a)}$	$g_{abs}^{b)}$	$\Delta g_{abs}^{c)}$	$\Delta g/g^{(v)}$ [%] ^{d)}	
YPCr	CP ^{e)}	x	390	8.03	1.45	6.58	0.55	0.37	0.18	0.44	0.12	0.32	73	this work
		x	460	-12.1	-0.19	-11.91	0.53	0.27	0.26	-0.69	-0.02	-0.67	97	
PProDOT-(2S-thylhexyl) ₂ ^{g)}	CP	x	620	1300	100	1200	1.3	0.5	0.8	30.0	6.1	24.0	80	5
		x	570	600	200	400	1.1	0.6	0.5	16.6	10.0	6.4	39	
Poly [(R)-BEDOT-(OCT*) ^{h)}	EP ^{f)}	x	450	12	2	10	0.15	0.3	-0.15	2.4	0.20	2.2	92	6
PEDOT ⁱ⁾	EP	o	450	500	50	450	0.5	0.25	0.25	30.0	6.0	24.0	80	7
PEDOT ^{j)}	EP	o	450	35	0	35	1.05	0.65	0.4	1.0	-0.0	1.0	100	8
Polyaniline ^{k)}	CP	o	440	60	0	60	1.8	0.8	1	1.0	-0.00	1.0	100	9
(R)-PBTh ^{l)}	EP	o	592	110	-10	120	0.6	0.7	-0.1	5.6	-0.43	6.0	108	10
PEDOT ^{m)}	EP	o	660	500	-750	1250	0.76	0.74	0.02	20.0	-31.0	51.0	254	11
Polyaniline ⁿ⁾	EP	o	470	550	100	450	0.7	0.8	-0.1	24.0	3.8	20.2	84	12
Thiophene-phenyl copolymer ^{o)}	EP	o	570	-150	50	-200	0.35	0.45	-0.1	-13.0	3.4	-16.0	126	13

The properties ^{a)} at the neutral state and ^{b)} at the oxidized state. ^{c)} The difference between the neural state and the oxidized state. ^{d)} The normalized anisotropy factor was determined by dividing Δg_{abs} by the g_{abs} at the neutral state. ^{e)} Polymers were synthesized by chemical polymerization or ^{f)} electrochemical polymerization. ^{g)} Chemically doped by I₂ vapor. ^{h)} Electrochemically doped from -0.7 to +0.7 V. ⁱ⁾ Electrochemically doped from -0.8 to 0.9 V. ^{j)} Electrochemically doped from -0.7 to +0.7 V. ^{k)} Dedoped by NH₄OH, and redoped by HCl. ^{l)} Electrochemically doped from 0.1 to 1.3V. ^{m)} Electrochemically doped from -0.45 to +0.64 V. ⁿ⁾ Electrochemically doped from 0.70 to 0.95V. ^{o)} Electrochemically doped from 0 to 1 V

Table S3. Coloration efficiency (CE) of the YPCr EC device with different switching potentials*:

(a) CE of the as-prepared YPCr film.

Potential [V]	ΔOD	Q [C/cm ²] x10 ⁻³	CE [cm ² /C]
-1	0.49	1.1	434
-0.5	0.48	1.1	454
0	0.47	1.0	454
0.3	0.47	1.0	457
zd0.5	0.47	1.0	462
0.7	0.32	0.85	377
0.8	0.17	0.53	323
0.9	0.07	0.30	230

(b) CE of the YPCr film after annealing at 120°C

Potential [V]	ΔOD	Q [C/cm ²] x10 ⁻³	CE [cm ² /C]
-1	0.43	0.82	5233
-0.5	0.43	0.71	601
0	0.43	0.70	617
0.3	0.44	0.70	631
0.5	0.44	0.70	631
0.7	0.30	0.53	569
0.8	0.16	0.31	516
0.9	0.05	0.16	323

*CE was determined by dividing the absorbance change (ΔOD) by the injected/ejected charge per unit area (Q). The ΔOD of the devices were monitored at 425 nm with a step potential of +1 V to the various dedoping potentials.

Table S4. Coloration efficiency (CE) of the YPCr EC device with different thicknesses.*(a) Absorbance change (ΔOD) at 425 nm of the YPCr films.

Potential [V]	$\Delta OD^a)$	$\Delta OD^b)$	$\Delta OD^c)$	$\Delta OD^d)$	$\Delta OD^e)$
-1	0.43	0.37	0.25	0.22	0.096
0	0.43	0.37	0.24	0.21	0.096
0.3	0.44	0.36	0.24	0.19	0.092
0.5	0.44	0.35	0.23	0.19	0.093
0.7	0.30	0.25	0.12	0.092	0.041
0.9	0.05	0.04	0.025	0.011	0.008

(b) The injected/ejected charge per unit area (Q) of the YPCr films during coloration.

Potential [V]	$Q^a)$ [C/cm ²] $\times 10^{-4}$	$Q^b)$ [C/cm ²] $\times 10^{-4}$	$Q^c)$ [C/cm ²] $\times 10^{-4}$	$Q^d)$ [C/cm ²] $\times 10^{-4}$	$Q^e)$ [C/cm ²] $\times 10^{-4}$
-1	8.2	7.1	6.7	6.6	6.2
0	7.0	5.9	5.4	5.6	3.4
0.3	7.0	5.5	4.6	4.2	3.3
0.5	7.0	5.1	4.1	3.4	2.9
0.7	5.3	4.2	2.8	2.2	1.7
0.9	1.6	1.3	1.3	0.8	0.4

(c) CE of the YPCr films

Potential [V]	CE ^{a)} [cm ² /C]	CE ^{b)} [cm ² /C]	CE ^{c)} [cm ² /C]	CE ^{d)} [cm ² /C]	CE ^{e)} [cm ² /C]
-1	524	521	377	327	155
0	614	627	451	367	284
0.3	629	655	522	457	276
0.5	629	687	563	561	322
0.7	566	595	440	422	246
0.9	313	308	195	143	223

*YPCr film thickness was ^{a)}180 nm, ^{b)}140 nm, ^{c)}80nm, ^{d)}50 nm, and ^{e)}20 nm. CE = $\Delta OD/Q$ at 425 nm.

Reference for supporting information

1. Oeda, Y.; Nishi, O.; Matsushima, Y.; Mizuno, K.; Matsui, A. H.; Michinomae, M.; Takeshima, M.; Goto, T. Exciton scattering, κ selection rule, exciton bandwidth in pyrene microcrystallites, and lattice relaxation energy for the origin of V luminescence. *Chem. Phys.* 1996, 213, 421-427.
2. Bhuvana, T.; Kim, B.; Yang, X.; Shin, H.; Kim, E. Reversible Full-Color Generation with Patterned Yellow Electrochromic Polymers. *Angew. Chem. Int. Ed.* 2013, 52, 1180-1184.
3. Bhuvana, T.; Kim, B.; Yang, X.; Shin, H.; Kim, E. Electroactive subwavelength gratings (ESWGs) from conjugated polymers for color and intensity modulation. *Nanoscale* 2012, 4, 3679-86.
4. Amb, C. M.; Kerszulis, J. A.; Thompson, E. J.; Dyer, A. L.; Reynolds, J. R. Propylenedioxythiophene (ProDOT)-phenylene copolymers allow a yellow-to-transmissive electrochrome. *Polymer Chemistry* 2011, 2, 812.
5. Grenier, C. R. G.; George, S. J.; Joncheray, T. J.; Meijer, E. W.; Reynolds, J. R. Chiral Ethylhexyl Substituents for Optically Active Aggregates of π -Conjugated Polymers. *J. Am. Chem. Soc.* 2007, 129, 10694-10699.
6. Jeong, Y. S.; Goto, H.; Iimura, S.; Asano, T.; Akagi, K. Chiral BEDOT-based copolymers prepared by chemical and electrochemical polymerization. *Curr. Appl. Phys.* 2006, 6, 960-963.
7. Goto, H. Vortex fibril structure and chiroptical electrochromic effect of optically active poly(3,4-ethylenedioxythiophene) (PEDOT*) prepared by chiral transcription electrochemical polymerisation in cholesteric liquid crystal. *J. Mater. Chem.* 2009, 19, 4914.
8. Jeong, Y. S.; Akagi, K. Control of Chirality and Electrochromism in Copolymer-Type Chiral PEDOT Derivatives by Means of Electrochemical Oxidation and Reduction. *Macromolecules* 2011, 44, 2418-2426.
9. Pornputtkul, Y.; Kane-Maguire, L. A. P.; Wallace, G. G. Influence of Electrochemical Polymerization Temperature on the Chiroptical Properties of (+)-Camphorsulfonic Acid-Doped Polyaniline. *Macromolecules* 2006, 39, 5604-5610.
10. Goto, H.; Akagi, K. Asymmetric Electrochemical Polymerization: Preparation of Polybithiophene in a Chiral Nematic Liquid Crystal Field and Optically Active Electrochromism. *Macromolecules* 2005, 38, 1091-1098.
11. Goto, H.; Akagi, K. Optically Active Electrochromism of Poly(3,4-ethylenedioxythiophene) Synthesized by Electrochemical Polymerization in Lyotropic Liquid Crystal of Hydroxypropyl Cellulose/Water: Active Control of Optical Activity. *Chem. Mater.* 2005, 18, 255-262.
12. Zhang, X.; Song, W. Potential controlled electrochemical assembly of chiral polyaniline with enhanced stereochemical selectivity. *Polymer* 2007, 48, 5473-5479.
13. Goto, H. Doping-Dedoping-Driven Optic Effect of π -Conjugated Polymers Prepared in Cholesteric-Liquid-Crystal Electrolytes. *Phys. Rev. Lett.* 2007, 98, 253901.